

Mesoporous Microspheres with Doubly Ordered Core–Shell Structure

Adolfo López-Noriega,[†] Eduardo Ruiz-Hernández,[†]
Sam M. Stevens,^{‡,§} Daniel Arcos,[†]
Michael W. Anderson,[‡] Osamu Terasaki,[§] and
Maria Vallet-Regí^{†*}

Dpto. Química Inorgánica y Bioinorgánica Facultad de Farmacia, Universidad Complutense de Madrid and Networking Research Center on Bioengineering, Biomaterials and Nanomedicine, (CIBER-BBN), Plaza Ramón y Cajal s/n, 28040, Madrid, Spain, Centre for Nanoporous Materials, School of Chemistry, University of Manchester, Oxford Road, Manchester M13 9PL, United Kingdom, and Arrhenius Laboratory, Stockholm University, S-10691 Stockholm, Sweden

Received October 21, 2008

Revised Manuscript Received November 10, 2008

Current needs in catalysis and controlled release of therapeutic agents have triggered an intensive quest in the design of porous materials with mesoscale structure. Monoliths, fibers, nanotubes, or thin films showing mesoporosity have been synthesized in the past few years. Spheres are one of the most investigated morphologies due to their suitability for a great number of applications.¹ There are several methods for obtaining mesoporous materials as microspheres, among them, the so-called modified Stöber method,² based on the condensation of silica under a basic medium in the presence of a cationic structure directing agent, is a well-known synthetic process yielding monodisperse microspheres with diverse mesoporous arrangements. On the other hand, aerosol-assisted method permits using not only cationic but also anionic and nonionic surfactants for achieving mesoporous microspheres,³ thus facilitating the many different pore sizes and organizations. Many research groups have considered using core–shell structures based on mesoporous microspheres. Recently, materials with different hydrophilic profiles between core and shell components but with a uniform pore size were synthesized by Yano et al. Furthermore, mesoporous shells have been added to

hollow and solid silica core microspheres or to magnetic nanoparticles covered by amorphous silica.⁴

To the best of our knowledge, this work describes for the first time the synthesis of core–shell silica based microspheres showing different ordered mesoporous arrangements in core and shell. The combination of two versatile synthetic routes gives rise to materials with a hierarchically organized porous structure, in which a wide variety of core–shell networks could be developed. Additionally, this system is compatible with readily available functionalization pathways, opening the possibility of producing a range of fine-tuned devices.

Silica core–shell double mesoporous microspheres (DMM) were synthesized following a two step procedure. First, core mesoporous microspheres were made using an aerosol-assisted process in the presence of nonionic surfactant, Pluronic P123 [(ethylene oxide, EO)₂₀(propylene oxide, PO)₇₀(EO)₂₀], as the structure directing agent. Tetraethoxysilane ([Si(OCH₂CH₃)₄], TEOS) was used as the SiO₂ precursor. The precursor solution was prepared by solving 8.13 g of P123 in 900 mL of ethanol and 51.13 mL of water (for DMM) or a ferrofluid (in the case of γ -DMM). This solvent composition was chosen on the basis that alcohol-rich solutions lead to better organized mesostructures compared with water-rich ones during spray-drying processes.⁵ The pH of this solution was adjusted to 1.2 by the addition of 6 M HNO₃. Once P123 was completely solved, 43.44 mL of TEOS was added and the whole system stirred overnight. The aerosol was generated by a piezoelectric device placed at the bottom of the vessel containing the precursor solution. Near its own resonance frequency, the piezoelectric device forms a geyser in the surface of the liquid and ultrafine droplets are produced. This aerosol is conveyed by N₂ to the preheating zone (where self-assembly of silica and the surfactant takes place) and afterward to the pyrolysis zone (65 cm tubular furnace at 400 °C). Dried particles are collected in an electrostatic filter. Powder obtained from this aerosol-assisted process is calcined at 425 °C for 3 h in air in order to remove the surfactant. In order to check the suitability of this method for encapsulating nanoparticle-loaded materials, core mesoporous microspheres containing maghemite (γ -Fe₂O₃) nanoparticles were also covered following the same procedure^{3c} and the resultant material was denoted γ -DMM.

Second, mesoporous shells encapsulating the core microspheres were added to the materials by means of a modified Stöber process with CTAB as structure directing agent. The mesoporous shell was formed by performing the modified

[†] Universidad Complutense de Madrid and Networking Research Center on Bioengineering, Biomaterials and Nanomedicine.

[‡] University of Manchester.

[§] Stockholm University.

- (1) (a) Davis, M. E. *Nature* **2002**, *417*, 813. (b) Huo, Q.; Zhao, D. Y.; Feng, J. L.; Weston, K.; Buratto, S. K.; Stucky, G. D.; Schacht, S.; Schüth, F. *Adv. Mater.* **1997**, *9*, 974. (c) Wu, X. W.; Ruan, J. F.; Ohsuna, T.; Terasaki, O.; Che, S. N. *Chem. Mater.* **2007**, *19*, 1577. (d) Lu, Y. F.; Ganguli, R.; Drewien, C. A.; Anderson, M. T.; Brinker, C. J.; Gong, W. L.; Guo, Y. X.; Soyez, H.; Dunn, B.; Huang, M. H.; Zink, J. I. *Nature* **1997**, *389*, 364.
- (2) (a) Stöber, W.; Fink, A.; Bohn, E. *J. Colloid Interface Sci.* **1968**, *26*, 62. (b) Grun, M.; Lauer, I.; Unger, K. K. *Adv. Mater.* **1997**, *9*, 254.
- (3) (a) Lu, Y. F.; Fan, H. Y.; Stump, A.; Ward, T. L.; Rieker, T.; Brinker, C. J. *Nature* **1999**, *398*, 223. (b) Brinker, C. J.; Lu, Y. F.; Sellinger, A.; Fan, H. Y. *Adv. Mater.* **1999**, *11*, 579. (c) Ruiz-Hernández, E.; López-Noriega, A.; Arcos, D.; Izquierdo-Barba, I.; Terasaki, O.; Vallet-Regí, M. *Chem. Mater.* **2007**, *19*, 3455. (d) Areva, S.; Boissière, C.; Grosso, D.; Asakawa, T.; Sanchez, C.; Lindén, M. *Chem. Commun.* **2004**, 1630.

- (4) (a) Yano, K.; Nakamura, T. *Chem. Lett.* **2006**, *35*, 1014. (b) Chang-Chien, C. Y.; Hsu, C. H.; Lee, T. Y.; Liu, C. W.; Wu, S. H.; Lin, H. P.; Tang, C. Y.; Lin, C. Y. *Eur. J. Inorg. Chem.* **2007**, *24*, 3798. (c) Yoon, S. B.; Kim, J.-Y.; Kim, J. H.; Park, Y. J.; Yoon, K. R.; Park, S.-K.; Yu, J.-S. *J. Mater. Chem.* **2007**, *17*, 1758. (d) Deng, Y.; Qi, D.; Deng, C.; Zhang, X.; Zhao, D. *J. Am. Chem. Soc.* **2008**, *130*, 28. (e) Julian-Lopez, B.; Boissière, C.; Chaneac, C.; Grosso, D.; Vasseur, S.; Miroux, S.; Duguet, E.; Sanchez, C. *J. Mater. Chem.* **2007**, *17*, 1563.
- (5) Boissière, C.; Grosso, D.; Amenitsch, H.; Gibaud, A.; Coupé, A.; Baccile, N.; Sanchez, C. *Chem. Commun.* **2003**, 2798.

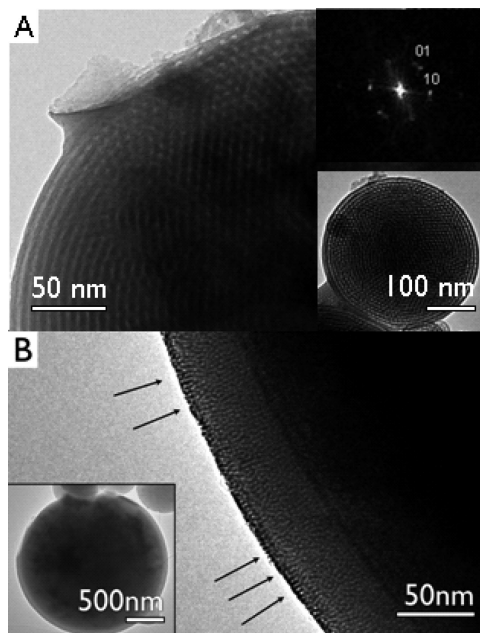


Figure 1. TEM images of maghemite loaded core (A) and core-shell microspheres γ -DMM (B). Arrows indicating shell mesoporous channels orientation.

Stöber process in the presence of the core microspheres. A total of 500 mg of aerosol-synthesized material was added to a solution of 298 mg of CTAB in ethanol/water (0.4:1, molar). This solution was brought to pH = 11.5 by the addition of NH_3 (25%) and stirred for 15 min. Under this pH conditions, there is a risk of partial dissolution of the silica core, which seems to be inhibited by the addition of CTAB. Afterward, 613 μL of TEOS were added dropwise under vigorous stirring while evaporation of ammonia from the solution was prevented by sealing the beaker. The resultant suspension was stirred for 2 h and subsequently allowed to settle. The powder was recovered after centrifugation of the solution. The material was washed with water several times, centrifuged, and then dried at 60 $^\circ\text{C}$ overnight. The microspheres were finally calcined at 425 $^\circ\text{C}$ for 3 h in air.

In the core microspheres, that is, those synthesized by aerosol assisted method before coating, a two-dimensional hexagonal arrangement is identified (Figure 1A). However, DMMs exhibit a core-shell arrangement in which the inner and outer mesoporous structures display different hexagonal arrays (Figure 1B). Two phases can be clearly distinguished in TEM images, which is consistent with XRD patterns obtained from DMMs. These results evidence a hexagonal phase corresponding to the core and an additional phase with different cell parameters thus assignable to the shell component (continuous line in Figure 2).

The coating through modified Stöber process does not affect the integrity of those mesoporous cores containing maghemite nanoparticles. These can be still observed inside the spheres in the case of γ -DMM (with darker contrast in the inset of Figure 1B). Further XRD studies and magnetic properties analysis (saturation magnetization and coercive force values) of the coated γ -DMM evidenced that the

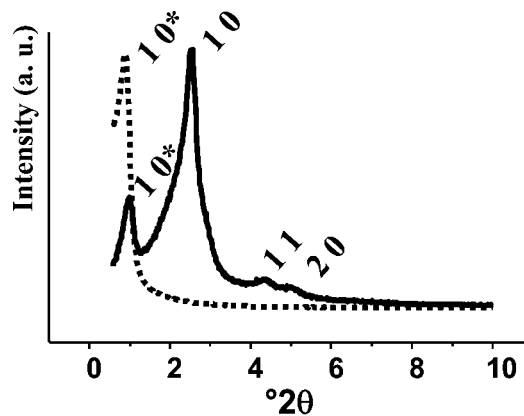


Figure 2. Small angle XRD patterns of core microspheres (dotted line) and core shell microsphere (continuous line).

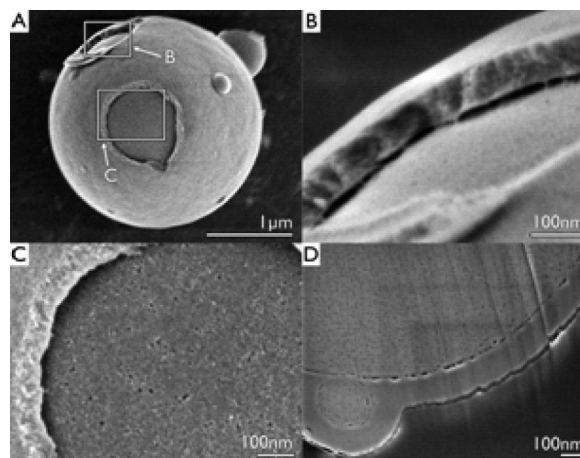


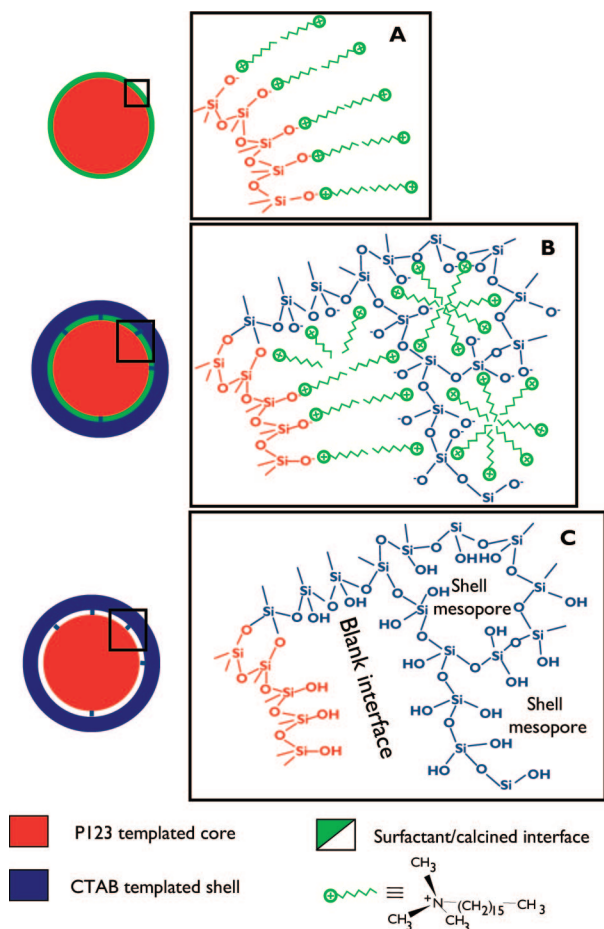
Figure 3. HRSEM micrographs of a crushed core-shell DMM microsphere (A, B, and C) and of cross-section polished material (D).

crystallochemical features and superparamagnetism of maghemite nanoparticles are preserved after the synthesis (see Supporting Information).

Although some isolated MCM-41 type microspheres could be observed after the shell formation by the Stöber method, most of the material resulting from the synthetic procedure detailed in this work presented a core-shell structure. At this point, it must be highlighted that when we tried to coat the cores without previous surface functionalization with CTAB, the resulting product was a mixture of noncoated aerosol-assisted microparticles together with smaller nanospheres formed through the common Stöber method (see Figure S6 in Supporting Information). This fact indicates that the core-shell formation mechanism competes with the particle formation described by Stöber, and the previous core functionalization with a surfactant is required for the subsequent shell formation.

High resolution scanning electron microscopy (HRSEM) images provide very clear information about the morphological characteristics of this system. Some DMMs were softly milled in order to partially crush the coatings (Figure 3A). In this way we could carry out observations directly over the core-shell interface. The core and shell mesoporous components appear to be connected through a columnar interface, which can be distinguished between the mesoporous phases (Figure 3B). Also some accessible pores can be

Scheme 1. Formation Route of Core–Shell Microspheres



observed on the surface of the inner spheres (Figure 3C). In order to more clearly observe the interconnection between core and shell, cross-section polishing (CP) using an argon ion beam⁶ was carried out on the materials. According to TEM, HRSEM, and CP-HRSEM results core microspheres are fully covered by the mesoporous layer which is from 40 to 100 nm wide. The HRSEM image, Figure 3D, shows that the interface is a space of a few nanometers in size with randomly distributed silica columns created during the modified Stöber process.

The core–shell type microstructure, as well as the connectivity between both components, can be explained in terms of an electrostatic interactions mechanism, during the microspheres coating. The surface of the silica core is negatively charged during the shell synthesis. In these conditions cationic surfactant molecules would create a layer over the surface of the core microspheres (Scheme 1A). This layer would be responsible for the eventual mesoscale core–shell gaps, templating the silica columns among both phases (Scheme 1B) through further condensation of the core silica with the new silica species added during the Stöber process. The condensation of the new silica network and the assembly with the surfactant may take place around this

layer. The calcination process removes both the layer of surfactant at the core–shell interface and the surfactant within the coating pores, achieving the outer mesoporous shell (Scheme 1C). This mechanism based on electrostatic interactions is confirmed by the fact that no further assembly is found when CTAB is not present during the synthesis, therefore leading to independent dense silica spheres resulting from Stöber condensation.

A careful micrograph observation allows the fact that the gap seems to be larger than the 3 nm expected by the surfactant bilayer considered in the Scheme 1 to be seen. This additional enlargement could be due to the different thermal contraction of the core and the shell. The core has been previously treated at 425 °C before the gap formation, whereas the shell undergoes a first thermal treatment during the CTAB calcination. The higher silica condensation within the shell during the gap formation would explain the larger gap with respect to that expected from the surfactant bilayer.

TEM observations evidence that mesopores from the shell component are oriented radially in relation to the inner microspheres. Radially distributed outer mesopores would permit the flow of external fluids toward the mesoporous core. The radial distribution of the outer pores is in accord with previous studies on modified Stöber syntheses.^{4,7} This arrangement of the shell pores indicates that a seed growth mechanism is occurring during the shell formation. In our case, the core microspheres act as nucleation seeds of the silica-micelle aggregates that eventually form the shell. Further studies using cores with other mesopore structure (lamellar, worm-like, etc.) would be very interesting to test the influence on the gap and the shell. In addition, the use of ionic surfactants with longer chains and different concentrations also opens new possibilities for this system. For instance, longer chains would lead to larger gaps, whereas higher CTAB concentrations would increase the shell surface and porosity, although a gap enlargement would not occur, taking into account the bilayer formation considered in our model. In conclusion, the double ordering mesostructure of the microspheres provides unique features and new perspectives in the field of selective size sieves with application for heterogeneous catalysis processes.

Acknowledgment. Financial support of CICYT Spain through Research Project MAT2005-01486, CAMS-0505/MAT/000324, the Knut and Alice Wallenbergs Foundation and VR: Sweden and JST Japan (O.T.) and EPSRC are acknowledged. We thank Dr. I. Izquierdo-Barba for help in microscopy, Dr. F. Conde (CAI XRD, UCM), Dr. Y. Sakamoto, and Dr. F. Balas for fruitful discussion.

Supporting Information Available: N₂ adsorption porosimetry of DMM, XRD pattern of γ -DMM, magnetic characterization of γ -DMM, SEM analysis of DMM and γ -DMM, and TEM analysis of DMM and γ -DMM (PDF). This material is available free of charge via the Internet at <http://pubs.acs.org>.

CM8028565

(6) Takahashi, H.; Sato, A.; Takakura, M.; Mori, N.; Boerder, J.; Knoll, W.; Critchell, J. *Microchim. Acta* **2006**, 155, 295.

(7) Lebedev, O. I.; Van Tendeloo, G.; Collart, O.; Cool, P.; Vansant, E. F. *J. Solid State Sci.* **2004**, 6, 489.